Inorg. Chem. **2003**, *42*, 3308–3317

Synthesis of Lateral Macrobicyclic Compartmental Ligands: Structural, Magnetic, Electrochemical, and Catalytic Studies of Mono- and Binuclear Copper(II) Complexes

M. Thirumavalavan, P. Akilan, and M. Kandaswamy*

Department of Inorganic Chemistry, University of Madras, Guindy Campus, Chennai 600 025, India

Kandaswamy Chinnakali and G. Senthil Kumar

Department of Physics, Anna University, Chennai 600 025, India

H. K. Fun

X-ray Crystallography Unit, School of Physics, Universiti Sains Malaysia, 11800 USM, Penang, Malaysia

Received October 17, 2002

A series of putative mono- and binuclear copper(II) complexes, of general formulas $[CuL](ClO_4)$ and $[Cu_2L](ClO_4)_2$, respectively, have been synthesized from lateral macrocyclic ligands that have different compartments, originated from their corresponding precursor compounds (PC-1, 3,4:9,10-dibenzo-1,12-[*N*,*N*′-bis{(3-formyl-2-hydroxy-5-methyl)-benzyl}diaza]-5,8-dioxacyclotetradecane; and PC-2, 3,4:9,10-dibenzo-1,12-[*N*,*N*′-bis{(3-formyl-2-hydroxy-5-methyl)-benzyl}diaza]-5,8-dioxacyclopentadecane). The precursor compound PC-1 crystallized in the triclinic system with space group $P\bar{1}$. The mononuclear copper(II) complex $[CuL^{1a}](ClO_4)$ is crystallized in the monoclinic system with space group $P2_1/c$. The binuclear copper(II) complex $[Cu_2L^{2c}](ClO_4)_2$ is crystallized in the triclinic system with space group $P\bar{1}$; the two Cu ions have two different geometries. Electrochemical studies evidenced that one quasi-reversible reduction wave ($E_{pc} = -0.78$ to -0.87 V) for mononuclear complexes and two quasi-reversible one-electron-transfer reduction waves ($E^1_{pc} = -0.83$ to -0.92 V, $E^2_{pc} = -1.07$ to -1.38 V) for binuclear complexes are obtained in the cathodic region. Room-temperature magnetic-moment studies convey the presence of antiferromagnetic coupling in binuclear complexes [$\mu_{eff} = (1.45–1.55)\mu_B$], which is also suggested from the broad ESR spectra with $g = 2.10–2.11$, whereas mononuclear complexes show hyperfine splitting in ESR spectra and they have magnetic-moment values that are similar to the spin-only value [$\mu_{eff} = (1.69–1.72)\mu_B$]. Variable-temperature magnetic susceptibility study of the complex shows that the observed $-2J$ value for the binuclear complex $[Cu_2L^{1b}](ClO_4)_2$ is 214 cm^{-1}. The observed initial rate-constant values of catechol oxidation, using complexes as catalysts, range from 4.89×10^{-3} to 5.32×10^{-2} min^{-1} and the values are found to be higher for binuclear complexes than for the corresponding mononuclear complexes.

1. Introduction

Synthesis and characterization of novel phenoxo complexes are of main interest; these complexes are portals in the field of copper coordination chemistry and are at the meeting point of the two fields of molecular magnetism and macrocyclic compounds.[1–3] These phenoxo copper(II) complexes are the beacon in modeling, and they serve as bioinorganic model compounds not only in enzymatic reactions, but also in catalytic synthetic oxidation reactions.[4–8] Hence, binuclear copper(II) complexes are of interest for

* Author to whom correspondence should be addressed. E-mail: mkands@yahoo.com.

(1) Fusi, V.; Llobet, A.; Mahia, J.; Micheloni, M.; Paoli, P.; Ribas, X.; Rossi, P. *Eur. J. Inorg. Chem*. **2002**, 987.
(2) Rodriguez, M.; Liobet, A.; Corbella, M.; Muller, P.; Uson, M. A.; Martell, A. E.; Reibenspies, J. *J. Chem. Soc., Dalton Trans*. **2002**, 2900.

10.1021/ic020633+ CCC: $25.00
Published on Web 04/11/2003

availing magnetostructural correlations and as useful model systems for catalysis. Several macromonocyclic complexes of ligands, containing ether oxygen and tertiary nitrogen, tertiary nitrogen, and phenolic oxygen as coordinating atoms, were reported in the literature.[9] Only a few bicyclic systems have been studied so far.[10] Metal ions, together with ligands, contain a variety of structural information that has attracted attention in the field of supramolecular chemistry, because of the self-assembly reaction. They exhibit switching ability; i.e., their structure and/or physical and chemical properties change, because of the input of some external information. One of the superior switching processes among them is electrochemical interconversion of the location of the Cu ion between Cu(I) and Cu(II).[11,12] By varying the pH also, the ions can be translocated from one compartment to another compartment. From these points of view, we have focused on metal complexes with multidentate ligands that contain various compartmental moieties,[13] to have a poignant understanding of the combined behavior of magnetic, catalytic, and molecular-switching properties.

The present work involves the synthesis of new macrobicyclic tricompartmental ligands that contain N and O donor atoms and their mono- and binuclear copper(II) complexes. The first compartment (N_2O_2) is comprised of two ether O atoms and two tertiary N atoms, the second compartment (N_2O_2) contains two tertiary N atoms and two phenolic O atoms, and the third compartment (N_2O_2) is composed of two phenolic O atoms and two imine N atoms. The special feature of this ligand is that the size of all compartments can be modified easily by varying the number of methylene groups (diamines/dibromoalkanes) in the ligand framework.

2. Experimental Section

Elemental analysis was conducted on a Carlo Erba model 1106 elemental analyzer. ^{1}H NMR spectra were recorded using a model FX-80-Q Fourier transition NMR spectrometer. Electronic spectral studies were conducted on a Hitachi model 320 spectrophotometer in the wavelength range of 200−800 nm. IR spectra were recorded on a Hitachi model 270-50 spectrophotometer on KBr disks in the wavenumber range of 4000−250 cm^{-1}. Mass spectra were obtained on a JEOL model DX-303 mass spectrometer, and the electrospray mass spectra of the complexes were recorded on a Micromass model Quatro II triple quadrupole mass spectrometer. Molar conductivity was measured with an Elico model SX 80 conductivity bridge, using a freshly prepared solution of the complex in CH_3CN. Cyclic voltammograms were obtained on a model CHI600A electrochemical analyzer. The measurements were conducted under oxygen-free conditions, using a three-electrode cell in which a glassy carbon electrode was the working electrode, a saturated Ag/AgCl electrode was the reference electrode, and platinum wire was used as the auxiliary electrode. A ferrocene/ferrocenium (1+) couple was used as an internal standard; the $E_{1/2}$ value of the ferrocene/ferrocenium (Fc/Fc^+) couple, under the experimental conditions, is 470 mV in dimethylformamide (DMF), and the ΔE_p value for Fc/Fc^+ is 70 mV. Tetra(*n*-butyl)ammonium perchlorate was used as the supporting electrolyte. The room-temperature magnetic moment was measured on a PAR model 155 vibrating sample magnetometer. X-band electron spin resonance (ESR) spectra were recorded at 25 °C on a Varian model EPR-E 112 spectrometer, using diphenylpicrylhydrazine (DPPH) as the reference. The catalytic oxidation of catechol to *o*-quinone by the complexes was studied in a 10^{-3} M acetonitrile solution. The reaction was followed spectrophotometrically by choosing the strongest absorbance at 390 nm and monitoring the increase in the absorbance at this wavelength as a function of time. A plot of $\log[A_\infty/(A_\infty - A_t)]$ versus time was made for each complex, and the initial rate constant for the catalytic oxidation was calculated.

2.1. Crystal Structure Determination. Accurate unit cell parameters and orientation matrixes were obtained by a least-squares fit of high-angle reflections (Mo Kα radiation) measured on a Siemens SMART CCD area detector, using the ω scan mode for the 3,4,9,10-dibenzo-1,12-[*N*,*N*′-bis{(3-formyl-2-hydroxy-5-methyl)-benzyl}diaza]-5,8-dioxacyclotetradecane (PC-1). Cell refinement and data reduction for the compound were performed using the SAINT program (Siemens, 1996). A total of 12 469 reflections were collected, resulting in 8207 independent reflections, of which 4512 had $I > 2\sigma(I)$; these reflections were considered to be observed reflections. The intensities were corrected for Lorentz and polarization effects. The structure was solved by a direct methods procedure, as implemented in the SHELXS 97 program (Sheldrick, 1997).[14] The positions of all the non-hydrogen atoms were included in the full-matrix least-squares refinement, using the SHELXL 97 program (Sheldrick, 1997).[15] The positions of all the H atoms were geometrically fixed at calculated positions, and they were allowed to ride on the corresponding non-hydrogen atoms. The final R-factor converged to 0.088; the maximum and minimum values of the electron densities in the final electron density map were 0.966 and −0.888 e·Å^{-3}, respectively.

Dark-green crystals of $[CuL^{1a}](ClO_4)$ and $[Cu_2L^{2c}](ClO_4)_2$, with dimensions of 0.38 mm × 0.38 mm × 0.20 mm and 0.32 mm × 0.14 mm × 0.12 mm, were used for indexing and intensity data collection on a Siemens Smart CCD diffractometer equipped with a normal-focus, 3-kW, sealed-tube X-ray source and graphite monochromated Mo Kα radiation ($\lambda = 0.71073$ Å) at 293 ± 2 and 183 ± 2 K, respectively. Empirical absorption corrections were applied for the compound, using the SADABS program for the Siemens area detector. The structure was solved by direct methods and refined using the SHELXTL program. All non-hydrogen atoms were refined with anisotropic displacement parameters. The H atoms were introduced in idealized positions and refined isotropically with a riding model. The final R-value of $[CuL^{1a}](ClO_4)$ was 0.062, and the electrodensity map contains maximum and minimum peak

(3) Gao, E.-Q.; Yang, G.-M.; Liao, D.-Z.; Jiang, Z.-H.; Yan, S.-P.; Wang, G.-L. *J. Chem. Res. Synop.* **1999**, 278.
(4) Kaim, W.; Rall, J. *Angew. Chem.* **1996**, *108*, 47.
(5) Kitajima, N.; Moro-Oka, Y. *Chem. Rev.* **1994**, *94*, 737.
(6) Kitajima, N. *Adv. Inorg. Chem.* **1992**, *38*, 1.
(7) Reim, J.; Werner, R.; Haase, W.; Krebs, B. *Chem.—Eur. J.* **1998**, *4*, 289.
(8) Geetha, K.; Tiwari, S. K.; Chakravarthy, A. R.; Ananthakrishnan, G. *J. Chem. Soc., Dalton Trans.* **1999**, 4463.
(9) Yinemura, M.; Usuki, Y.; Ohba, M.; Okawa, H. *J. Chem. Soc., Dalton Trans.* **2000**, 3624.
(10) Van Voggel, F. C.; Verboom, W.; Reinhoudt, D. N. *Chem. Rev.* **1994**, *94*, 279.
(11) Amendola, V.; Fabbrizzi, L.; Mangano, C.; Pallavicini, P. *Acc. Chem. Res.* **2001**, *43*, 488.
(12) Collin, J.-P.; Buchecker, C. D.; Gavina, P.; Molero, M. C. J.; Sauvage, J.-P. *Acc. Chem. Res.* **2001**, *34*, 477.
(13) Manonmani, J.; Thirumurugan, Ra.; Kandaswamy, M.; Narayanan, V.; Shanmuga Sundara Raj, S.; Ponnuswamy, M. N.; Shanmugam, G.; Fun, H. K. *Polyhedron* **2001**, *20*, 3039.
(14) Sheldrick, G. M. *SHELXS-97. Program for the Refinement of Crystal Structures*; University of Göttingen, Göttingen, Germany, 1997.
(15) Sheldrick, G. M. *SHELXL-97. Program for the Refinement of Crystal Structures*; University of Gottingen, Göttingen, Germany, 1997.

heights of 0.73 and −0.98 e·Å^{-3}, respectively. The final R value of $[Cu_2L^{2c}](ClO_4)_2$ was 0.1050, and the final electrodensity map contained maximum and minimum peak heights of 0.762 and −1.660 e·Å^{-3}, respectively.

2.2. Materials. 5-Methylsalicyladehyde,[16] 3-chloromethyl-5-methylsalicylaldehyde,[17] and 3,4:9,10-dibenzo-1,12-diaza-5,8-dioxacyclotetradecane[18,19] were prepared from the literature methods. Tetra(*n*-butyl)ammonium perchlorate (TBAP), used as the supporting electrolyte in electrochemical measurement, was purchased from Fluka and recrystallized from hot methanol. (Caution! TBAP is potentially explosive; hence, care should be taken in handling the compound.) DMF and CH_3CN were obtained from E. Merck.

Methanol is added sufficiently to acetonitrile fractionated at high reflux until the boiling temperature rises from 60 °C to 80 °C and the distillate becomes optically clear. Sodium hydride was added, and the mixture was refluxed for 15 min and then distilled rapidly.

DMF can be azeotropically distilled with benzene (10% v/v, previously dried over CaH_2) at atmospheric pressure: water and benzene distill at <80 °C. The liquid remaining in the distillation flask is dried further by adding $MgSO_4$. After the flask and its contents were shaken for 1 day, an additional amount of $MgSO_4$ is added and the DMF is distilled at a pressure of 15−20 mmHg.

All other chemicals and solvents were of analytical grade and used as received, without any further purification.

2.3. Synthesis of Precursor Compounds. 2.3.1. 3,4:9,10-Dibenzo-1,12-[*N*,*N*′-bis{(3-formyl-2-hydroxy-5-methyl}benzyl)-diaza]-5,8-dioxacyclotetradecane (PC-1). A mixture of 3,4:9,10-dibenzo-1,12-diaza-5,8-dioxacyclotetradecane (0.95 g, 3.2 mmol) and triethylamine (1.32 g, 6.4 mmol) in tetrahydrofuran (THF) was added slowly to a stirred solution of 3-chloromethyl-5-methyl salicylaldehyde (1.16 g, 6.4 mmol) in THF. After the addition was completed, the stirring was continued further for one more hour. The entire solution was then refluxed under a water bath for 3 h and was allowed to cool on standing at room temperature. Copious water was added to this solution, to dissolve any salt that may have been obtained. The required compound then was extracted in an organic medium, using chloroform. The extraction was repeated two or three times. A pale-yellow compound was obtained when the solvent was evaporated at room temperature (25 °C). Light-yellow crystals were obtained on recrystallization from chloroform. Yield: 1.82 g (80%); m.p., 100 °C. Anal. Calcd for $C_{36}H_{38}O_6N_2 \cdot CHCl_3$ (%): C, 60.50; H, 5.32; N, 3.92. Found (%): C, 60.72; H, 5.36; N, 3.98. IR data (ν, cm^{-1}): 1678 (ν(C═O), s), 3448 (ν(OH), br). ^{1}H NMR (δ ppm in $CDCl_3$): 10.0 (s, 2H, CHO protons), 7.0 (m, 12H, aromatic protons), 4.7 (m, 4H, methylene protons attached to an O atom), 3.8 (m, 4H, methylene protons attached to a N atom), 3.5 (s, 8H, benzylic protons), 2.3 (s, 6H, aromatic CH_3 protons). Mass (EI) *m*/*z*: 594 (m$^+$).

2.3.2. 3,4:9,10-Dibenzo-1,12-[*N*,*N*′-bis{(3-formyl-2-hydroxy-5-methyl}benzyl)diaza]-5,8-dioxacyclopentadecane (PC-2). The 3,4:9,10-dibenzo-1,12-[*N*,*N*′-bis{(3-formyl-2-hydroxy-5-methyl)-benzyl}diaza]-5,8-dioxacyclopentadecane compound (PC-2) can be prepared from the previously described procedure, using 3,4:9,10-dibenzo-1,12-diaza-5,8-dioxacyclopentadecane instead of 3,4:9,10-dibenzo-1,12-diaza-5,8-dioxacyclotetradecane. Yield: 1.98 g (85%); m.p., 112 °C. Anal. Calcd for $C_{37}H_{40}O_6N_2 \cdot CHCl_3$ (%): C, 60.98; H, 5.49; N, 3.84. Found (%): C, 61.02; H, 5.58; N, 3.88. IR data

Scheme 1. Synthesis of Macrocyclic Mono- and Binuclear Copper(II) Complexes

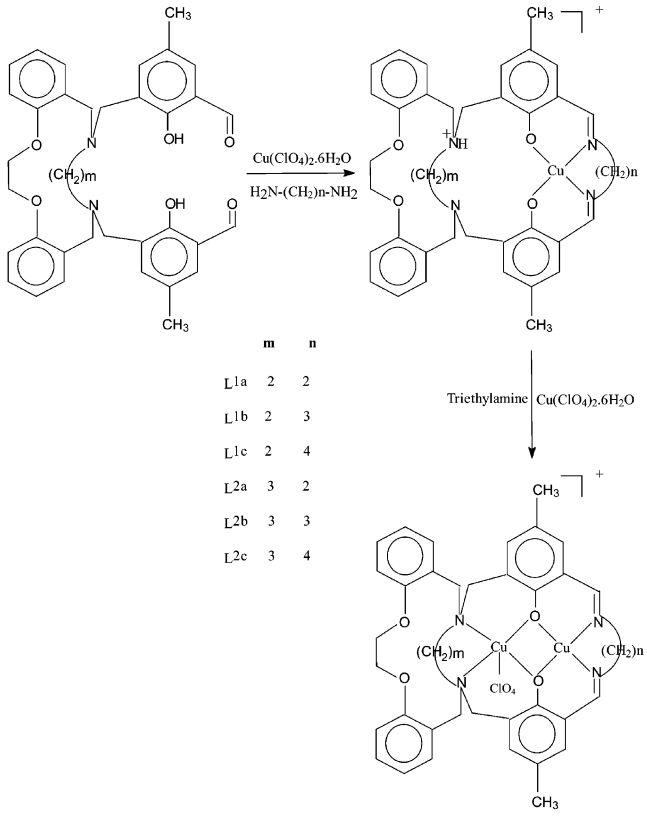

	m	n
L^{1a}	2	2
L^{1b}	2	3
L^{1c}	2	4
L^{2a}	3	2
L^{2b}	3	3
L^{2c}	3	4

(ν, cm^{-1}): 1677 (ν(C═O), s), 3435 (ν(OH), br). ^{1}H NMR (δ ppm in $CDCl_3$): 10.0 (s, 2H, CHO protons), 7.0 (m, 12H, aromatic protons), 4.5 (m, 4H, methylene protons attached to an O atom), 3.7 (m, 4H, methylene protons attached to a N atom), 3.5 (s, 8H, benzylic protons), 2.5 (s, 6H, aromatic CH_3 protons), 2.0 (s, 2H, CH_2 protons). Mass (EI) *m*/*z*: 608 (m$^+$).

2.4. Synthesis of Macrocyclic Mononuclear Copper(II) Complexes. 2.4.1. [CuL^{1a}](ClO$_4$). A methanolic solution of copper(II) perchlorate hexahydrate (0.676 g, 1.8 mmol) was added to the hot solution of PC-1 (1.085 g, 1.8 mmol) in $CHCl_3$, followed by the addition of 1,2-diaminoethane (0.121 g, 1.8 mmol) in methanol. The solution was refluxed in a water bath for 24 h. After the reaction was completed, the solution was filtered under hot conditions and allowed to cool on standing at room temperature. After slow evaporation of the solvent at 25 °C, a dark-green compound was obtained, washed with methanol, and dried under vacuum. The dark-green crystals were obtained on recrystallization from CH_3CN. Yield: 1.33 g (89%). Anal. Calcd for $C_{40}H_{44}O_8N_5ClCu$ (%): C, 58.39; H, 5.35; N, 8.51. Found (%): C, 58.46; H, 5.42; N, 8.62. Selected IR (KBr): 1630 (s), 1100 (s), 624 cm^{-1} (s). The conductance (Λ_m) in CH_3CN was 128 S·cm^2·mol^{-1}. λ_{max} (nm) (ϵ/M^{-1}·cm^{-1}) in CH_3CN: 580 (181), 350 (15 800), 280 (31 600). $g_{\|} = 2.31$, $g_{\perp} = 2.03$; $\mu_{eff} = 1.72$ μ_B.

The synthesis route of this complex, as well as that of the other mononuclear complexes, is shown in Scheme 1.

2.4.2. [CuL^{1b}](ClO$_4$). [CuL^{1b}](ClO$_4$) was synthesized by following the previously described procedure for [CuL^{1a}](ClO$_4$), using 1,3-diaminopropane instead of 1,2-diaminoethane. The compound obtained was dark green. Yield: 1.26 g (84%). Anal. Calcd for $C_{41}H_{46}O_8N_5ClCu$ (%): C, 58.85; H, 5.50; N, 8.37. Found (%): C, 58.94; H, 5.62; N, 8.41. Mass (EI) *m*/*z*: 795 (m$^+$). Selected IR (KBr): 1623 (s), 1096 (s), 625 cm^{-1} (s). Conductance in CH_3CN

(16) Duff, J. C. *J. Chem. Soc*. **1941**, 547.
(17) Crane, J. D.; Fenton, D. E.; Latour, J. M.; Smith, A. J. *J. Chem. Soc., Dalton Trans*. **1991**, 2279.
(18) Armstrong, L. G.; Lindoy, L. F. *Inorg. Chem*. **1975**, *14*, 1322.
(19) Grimsley, P. G.; Lindoy, L. F.; Lip, H. C.; Smith, R. J.; Baker, J. T. *Aust. J. Chem*. **1977**, *30*, 2095.

was given as $\Lambda_m = 135$ S·cm²·mol⁻¹. λ_{max} (nm) (ϵ/M⁻¹·cm⁻¹) in CH_3CN: 600 (193), 369 (12 300), 276 (62 400). $g_{||} = 2.29$, $g_{\perp} = 2.06$; $\mu_{eff} = 1.72$ μ_B.

2.4.3. [CuL^{1c}](ClO$_4$). [CuL^{1c}](ClO$_4$) was synthesized by following the previously described procedure for [CuL^{1a}](ClO$_4$), using 1,4-diaminobutane instead of 1,2-diaminoethane. The compound obtained was dark green. Yield: 1.26 g (82%). Anal. Calcd for $C_{42}H_{48}O_8N_5ClCu$ (%): C, 59.29; H, 5.64; N, 8.23. Found (%): C, 59.38; H, 5.72; N, 8.36. Selected IR (KBr): 1623 (s), 1096 (s), 627 cm^{-1} (s). Conductance in CH_3CN was given as $\Lambda_m = 156$ S·cm²·mol⁻¹. λ_{max} (nm) (ϵ/M⁻¹·cm⁻¹) in CH_3CN: 648 (152), 368 (15 500), 274 (45 700). $g_{||} = 2.22$, $g_{\perp} = 2.09$; $\mu_{eff} = 1.69$ μ_B.

2.4.4. [CuL^{2a}](ClO$_4$). The complex [CuL^{2a}](ClO$_4$) was synthesized by following the previously described procedure for [CuL^{1a}](ClO$_4$), but PC-2 was used in the preparation instead of PC-1. The compound obtained was dark green. Yield: 1.25 g (83%). Anal. Calcd for $C_{41}H_{46}O_8N_5ClCu$ (%): C, 58.85; H, 5.50; N, 8.37. Found (%): C, 58.96; H, 5.52; N, 8.42. Selected IR (KBr): 1620 (s), 1092 (s), 623 cm^{-1} (s). Conductance in CH_3CN was given as $\Lambda_m = 148$ S·cm²·mol⁻¹. λ_{max} (nm) (ϵ/M⁻¹·cm⁻¹) in CH_3CN: 595 (132), 369 (29 300), 273 (46 400). $g_{||} = 2.21$, $g_{\perp} = 2.03$; $\mu_{eff} = 1.71$ μ_B.

2.4.5. [CuL^{2b}](ClO$_4$). The complex [CuL^{2b}](ClO$_4$) was synthesized by following the previously described procedure for [CuL^{1b}](ClO$_4$), but PC-2 was used in the preparation instead of PC-1. The compound obtained was dark green. Yield: 1.23 g (80%). Anal. Calcd for $C_{42}H_{48}O_8N_5ClCu$ (%): C, 59.29; H, 5.64; N, 8.25. Found (%): C, 59.34; H, 5.69; N, 8.31. Selected IR (KBr): 1625 (s), 1100 (s), 620 cm^{-1} (s). Conductance in CH_3CN was given as $\Lambda_m = 160$ S·cm²·mol⁻¹. λ_{max} (nm) (ϵ/M⁻¹·cm⁻¹) in CH_3CN: 622 (120), 355 (22 400), 275 (32 100). $g_{||} = 2.22$, $g_{\perp} = 2.06$; $\mu_{eff} = 1.69$ μ_B.

2.4.6. [CuL^{2c}](ClO$_4$). The complex [CuL^{2c}](ClO$_4$) was synthesized by following the previously described procedure for [CuL^{1c}](ClO$_4$), but PC-2 was used in the preparation instead of PC-1. The compound obtained was dark green. Yield: 1.24 g (79%). Anal. Calcd for $C_{43}H_{50}O_8N_5ClCu$ (%): C, 59.72; H, 5.78; N, 8.10. Found (%): C, 59.78; H, 5.82; N, 8.16. Selected IR (KBr): 1624 (s), 1100 (s), 627 cm^{-1} (s). Conductance in CH_3CN was given as $\Lambda_m = 152$ S·cm²·mol⁻¹. λ_{max} (nm) (ϵ/M⁻¹·cm⁻¹) in CH_3CN: 640 (155), 363 (26 900), 278 (46 600). $g_{||} = 2.27$, $g_{\perp} = 2.07$; $\mu_{eff} = 1.72$ μ_B.

2.5. Synthesis of Macrocyclic Binuclear Copper(II) Complexes. 2.5.1. [Cu$_2$L^{1a}](ClO$_4$)$_2$. A methanolic solution of copper(II)perchlorate hexahydrate (0.676 g, 1.8 mmol) was added to the hot solution of PC-1 (1.085 g, 1.8 mmol) in $CHCl_3$, followed by the addition of 1,2-diaminoethane (0.121 g, 1.8 mmol) and triethylamine (0.251 g, 1.8 mmol) in methanol. Copper(II) perchlorate (0.676 g, 1.8 mmol) was added after 1 h, and the entire reaction mixture was refluxed in a water bath for 24 h. After the reaction was over, the reaction mixture was filtered and allowed to cool on standing at room temperature (25 °C). After slow evaporation of the solvent at 25 °C, the dark-green compound obtained was washed with methanol and dried under vacuum. Dark-green crystals were obtained on recrystallization from CH_3CN. Yield: 1.48 g (80%). Anal. Calcd for $C_{42}H_{46}O_{12}N_6Cl_2Cu_2$ (%): C, 49.26; H, 4.49; N, 8.21. Found (%): C, 49.31; H, 4.54; N, 8.29. Selected IR (KBr): 1628 (s), 1089, 1096, 1100 (w), 620 cm^{-1} (s). Conductance in CH_3CN was given as $\Lambda_m = 152$ S·cm²·mol⁻¹. λ_{max} (nm) (ϵ/M⁻¹·cm⁻¹) in CH_3CN: 575 (271), 372 (17 100), 272 (69 100). $g = 2.10$; $\mu_{eff} = 1.45$ μ_B.

The synthesis route for this complex and the other binuclear complexes is shown in Scheme 1.

2.5.2. [Cu$_2$L^{1b}](ClO$_4$)$_2$. [Cu$_2$L^{1b}](ClO$_4$)$_2$ was synthesized by following the previously described procedure for [Cu$_2$L^{1a}](ClO$_4$)$_2$, using 1,3-diaminopropane instead of 1,2-diaminoethane. The compound obtained was dark green. Yield: 1.47 g (78%). Anal. Calcd for $C_{43}H_{48}O_{12}N_6Cl_2Cu_2$ (%): C, 49.75; H, 4.62; N, 8.10. Found (%): C, 49.82; H, 4.69; N, 8.18. Selected IR (KBr): 1623 (s), 1089, 1096, 1100 (w), 623 cm^{-1} (s). Conductance in CH_3CN was given as $\Lambda_m = 148$ S·cm²·mol⁻¹. λ_{max} (nm) (ϵ/M⁻¹·cm⁻¹) in CH_3CN: 590 (257), 356 (21 300), 268 (70 000). $g = 2.11$; $\mu_{eff} = 1.49$ μ_B.

2.5.3. [Cu$_2$L^{1c}](ClO$_4$)$_2$. [Cu$_2$L^{1c}](ClO$_4$)$_2$ was synthesized by following the previously described procedure, using 1,4-diaminobutane instead of 1,2-diaminoethane. The compound obtained was dark green. Yield: 1.52 g (80%). Anal. Calcd for $C_{44}H_{50}O_{12}N_6Cl_2Cu_2$ (%): C, 50.23; H, 4.75, N, 7.99. Found (%): C, 50.29; H, 4.81; N, 8.07. Selected IR (KBr): 1624 (s), 1091, 1098, 1101 (w), 624 cm^{-1} (s). Conductance in CH_3CN was given as $\Lambda_m = 133$ S·cm²·mol⁻¹. λ_{max} (nm) (ϵ/M⁻¹·cm⁻¹) in CH_3CN: 628 (208), 349 (27 900), 272 (63 400). $g = 2.10$; $\mu_{eff} = 1.52$ μ_B.

2.5.4. [Cu$_2$L^{2a}](ClO$_4$)$_2$. The complex [Cu$_2$L^{2a}](ClO$_4$)$_2$ was synthesized by following the previously described procedure for [Cu$_2$L^{1a}](ClO$_4$)$_2$, but PC-2 was used in the preparation instead of PC-1. The compound obtained was dark green. Yield: 1.49 g (79%). Anal. Calcd for $C_{43}H_{48}O_{12}N_6Cl_2Cu_2$ (%): C, 49.75; H, 4.62; N, 8.10. Found (%): C, 49.81; H, 4.71; N, 8.21. Mass (EI) *m*/*z*: 955 (m$^+$). Selected IR (KBr): 1622 (s), 1086, 1096, 1100 (w), 624 cm^{-1} (s). Conductance in CH_3CN was given as $\Lambda_m = 160$ S·cm²·mol⁻¹. λ_{max} (nm) (ϵ/M⁻¹·cm⁻¹) in CH_3CN: 587 (228), 357 (16 700), 272 (63 000). $g = 2.10$; $\mu_{eff} = 1.46$ μ_B.

2.5.5. [Cu$_2$L^{2b}](ClO$_4$)$_2$. The complex [Cu$_2$L^{2b}](ClO$_4$)$_2$ was synthesized by following the previously described procedure for [Cu$_2$L^{1b}](ClO$_4$)$_2$, but PC-2 was used in the preparation instead of PC-1. The compound obtained was dark green. Yield: 1.44 g (76%). Anal. Calcd for $C_{44}H_{50}O_{12}N_6Cl_2Cu_2$ (%): C, 50.23; H, 4.75; N, 7.99. Found (%): C, 50.31; H, 4.83; N, 8.10. Selected IR (KBr): 1623 (s), 1088, 1096, 1101 (w), 625 cm^{-1} (s). Conductance in CH_3CN was given as $\Lambda_m = 155$ S·cm²·mol⁻¹. λ_{max} (nm) (ϵ/M⁻¹·cm⁻¹) in CH_3CN: 613 (248), 367 (11 200), 273 (27 300). $g = 2.11$; $\mu_{eff} = 1.51$ μ_B.

2.5.6. [Cu$_2$L^{2c}](ClO$_4$)$_2$. The complex [Cu$_2$L^{2c}](ClO$_4$)$_2$ was synthesized by following the previously described procedure for [Cu$_2$L^{1c}](ClO$_4$)$_2$, but PC-2 was used in the preparation instead of PC-1. The compound obtained was dark green. Yield: 1.48 g (77%). Anal. Calcd for $C_{45}H_{52}O_{12}N_6Cl_2Cu_2$ (%): C, 50.70; H, 4.88; N, 7.88. Found (%): C, 50.79; H, 4.93; N, 7.96. Selected IR (KBr): 1623 (s), 1085, 1098, 1102 (w), 627 cm^{-1} (s). Conductance in CH_3CN was given as $\Lambda_m = 129$ S·cm²·mol⁻¹. λ_{max} (nm) (ϵ/M⁻¹·cm⁻¹) in CH_3CN: 632 (266), 375 (19 900), 273 (23 500). $g = 2.11$; $\mu_{eff} = 1.55$ μ_B.

2.6. Yield of Macrocyclic Complexes. The yield of the macrocyclic complexes is moderately high, which is due to template synthesis involving simple Schiff's base condensation. The yield of the complexes varies only slightly from that of the others. Generally, the yield of the binuclear complexes is slightly less than that of the corresponding mononuclear complexes.

3. Results and Discussion

3.1. X-ray Structural Study of Precursor Compound 1 (PC-1). Figure 1 shows the ORTEP plot of precursor compound **1** (PC-1). Crystal data and structure refinement for PC-1 are given in Table 1. For C−N, the distance varies between 1.467 and 1.488 Å. No anomalous bond distances and bond angles were found in the structure, and all the bond distances and bond angles agree well with reported literature. The sum of the angle around the atoms N1 and N2 (N1 =

Table 1. Crystal Data and Structure Refinement for Precursor Compound PC-1, $[CuL^{1a}](ClO_4)$, and $[Cu_2L^{2c}](ClO_4)_2$

	precursor compound PC-1	$[CuL^{1a}](ClO_4)$	$[Cu_2L^{2c}](ClO_4)_2$
empirical formula	$C_{37}H_{39}Cl_3N_2O_6$	$C_{40}H_{44}ClCuN_5O_8$	$C_{45}H_{52}Cl_2Cu_2N_6O_{12}$
fw	714.05	821.79	1064.89
temp	293 ± 2 K	293 ± 2 K	183 ± 2 K
wavelength	0.71073 Å	0.71073 Å	0.71073 Å
cryst syst	triclinic	monoclinic	triclinic
space group	$P\bar{1}$	$P2_1/c$	$P\bar{1}$
a	9.0210(2) Å	21.3084(10) Å	10.2740(3) Å
b	13.6318(3) Å	11.8064(5) Å	12.2204(3) Å
c	14.9842(2) Å	15.6810(7) Å	18.6211(2) Å
α	93.2340(10)°	90°	94.521(2)°
β	107.05°	104.1720(10)°	93.691(2)°
γ	90.7600(10)°	90°	104.116(2)°
vol	1758.00(6) Å^3	3824.9(3) Å^3	2251.81(9) Å^3
Z	2	4	2
density (calculated)	1.349 Mg/m^3	1.427 Mg/m^3	1.571 Mg/m^3
abs coeff	0.309 mm^{-1}	0.701 mm^{-1}	1.134 mm^{-1}
F(000)	748	1716	1100
cryst size	0.20 mm × 0.28 mm × 0.42 mm	0.38 mm × 0.38 mm × 0.20 mm	0.32 mm × 0.14 mm × 0.12 mm
index ranges	$-12 \le h \le 11$, $-18 \le k \le 14$, $-14 \le l \le 19$	$-23 \le <h \le 25$, $-11 \le k \le 14$, $-16 \le l \le 18$	$-13 \le h \le 13$, $-11 \le k \le 16$, $-24 \le l \le 23$
reflns collected	12 469	20 293	13 671
independent reflns	8207 [R(int) = 0.0513]	6687 [R(int) = 0.134]	10 293 [R(int) = 0.1205]
refinement method	full-matrix least-squares on F^2	full-matrix least-squares on F^2	full-matrix least-squares on F^2
data/restraints/params	8207/0/444	6687/0/502	10 293/0/606
GOF on F^2	1.005	0.93	0.841
final R indexes [$I > 2\sigma(I)$]	R1 = 0.0884, wR2 = 0.2647	R1 = 0.062, wR2 = 0.154	R1 = 0.1050, wR2 = 0.2230
R indexes (all data)	R1 = 0.1318, wR2 = 0.2967	R1 = 0.102, wR2 = 0.167	R1 = 0.3081, wR2 = 0.3097
largest diff. peak and holes	0.966 and −0.888 e·Å^{-3}	0.73 and −0.98 e·Å^{-3}	0.762 and −1.660 e·Å^{-3}

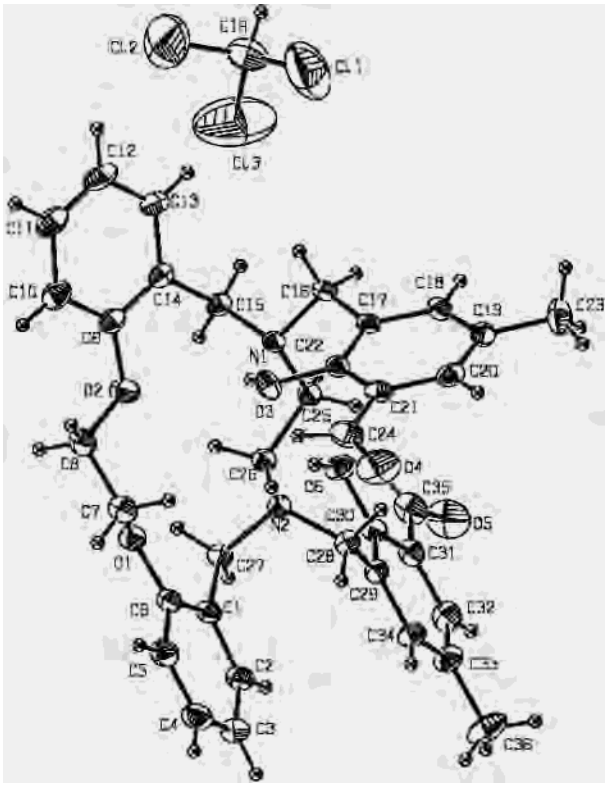

Figure 1. ORTEP diagram of the precursor compound PC-1, with atom labels and the numbering scheme. H atoms are omitted for clarity.

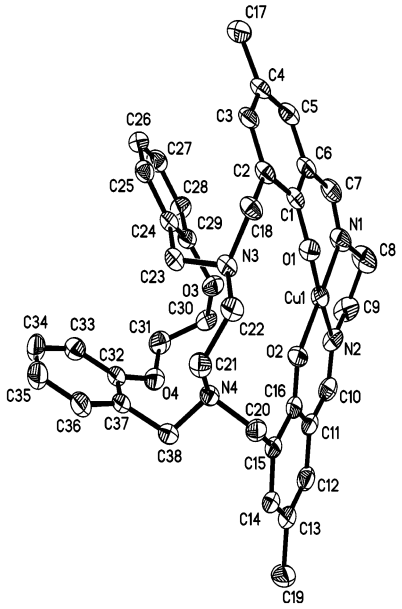

Figure 2. ORTEP diagram of the complex $[CuL^{1a}](ClO_4)\cdot CH_3CN$, showing the atom labeling scheme. All H atoms have been omitted for clarity.

333.0°, N2 = 335.5°) is indicative of sp3 hybridization. All the four phenyl rings are essentially planar, with a maximum deviation of 0.072(4) Å at c59. Rings A and D are almost coplanar; the dihedral angle between them is 10.0(7)°. Aside from the van der Waals interaction, the packing of the molecules is stabilized by two intermolecular C−H···O-type interactions [C1A−H1A...O6 (D−A = 3.261 Å; D−H···A = 158.3°; symmetry = 1 − *x*, −*y*, −*z*); C18−H21...O5 (D−A = 3.32 Å; D−H···A = 163.6°; symmetry = −*x*, 1 − *y*, −*z*)] and one C−H···*π*-type interaction [C12−H14...Cg (X...Cg = 3.538 Å; X−H···Cg = 160.5°; symmetry = 1 + *x*, *y*, *z*), Cg = Ring3].

3.2. X-ray Structural Study of the Mononuclear Complex $[CuL^{1a}](ClO_4)$. The molecular structure of the mononuclear copper(II) complex $[CuL^{1a}](ClO_4)$, along with atomic labeling, is given in Figure 2. Crystal data and structure refinement for the complex $[CuL^{1a}](ClO_4)$ are given in Table 1. Selected bond lengths and bond angles are summarized in Table 2. The Cu(II) ion in the complex is four-coordinated, and the geometry around the copper nuclei is best described as distorted square planar. Two imine N atoms and two phenoxy O atoms were coordinated in the equatorial plane to the Cu ion at distances of Cu(1)−O(1) = 1.883(3), Cu-

Table 2. Selected Bond Lengths and Angles for $[CuL^{1a}](ClO_4)^a$

Bond Lengths (Å)			
Cu(1)−O(1)	1.883(3)	Cu(1)−N(1)	1.928(4)
Cu(1)−O(2)	1.887(3)	Cu(1)−N(2)	1.931(3)
Bond Angles (deg)			
O(1)−Cu(1)−O(2)	88.06(12)	O(1)−Cu(1)−N(1)	177.15(15)
O(1)−Cu(1)−N(1)	93.33(14)	O(2)−Cu(1)−N(2)	94.18(14)
O(2)−Cu(1)−N(1)	177.99(14)	N(1)−Cu(1)−N(2)	84.48(16)

[a] Numbers in parentheses are estimated standard deviations in the least significant digits.

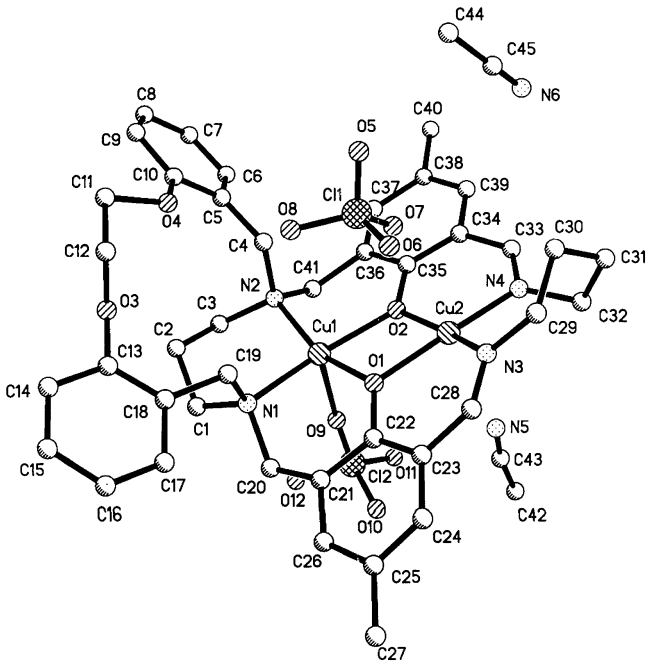

Figure 3. ORTEP diagram of complex $[Cu_2L^{2c}](ClO_4)_2 \cdot 2CH_3CN$, showing the atom labeling scheme. All H atoms have been omitted for clarity.

(2)−O(2) = 1.887(3), Cu(1)−N(1) = 1.928(4), and Cu(1)−N(2) = 1.931(3) Å, respectively. It is connoted that both oxygen atoms O1 and O2 are present at the same distance from the Cu atom and the nitrogen atoms N1 and N2 are present at the same distance from the Cu atom, within the experimental error. It was observed, in this macrocyclic complex, that one of the tertiary nitrogen atoms (N3 or N4) is protonated, as shown by the degree of pyramidalization. One perchlorate anion is present in the complex, and this ion neutralizes the positive charge of the complex. The acetonitrile molecule found in the crystal is not coordinated to the Cu(II) ion and occupies the crystal lattice as a free molecule. In the ORTEP diagram of the complex $[CuL^{1a}](ClO_4)$, the perchlorate anion and acetonitrile molecule are omitted for clarity.

3.3. X-ray Structural Study of the Binuclear Complex $[Cu_2L^{2c}](ClO_4)_2$. The molecular structure of the binuclear copper(II) complex $[Cu_2L^{2c}](ClO_4)_2 \cdot 2CH_3CN$, along with atomic labeling, is given in Figure 3. Crystal data and structure refinement for the complex $[Cu_2L^{2c}](ClO_4)_2 \cdot 2CH_3CN$ are given in Table 1. Selected bond lengths and bond angles are summarized in Table 3. The coordination around the Cu1 atom is distorted square pyramidal, with the basal plane occupied by two oxygen atoms (O1, O2) and two nitrogen atoms (N1, N2). The perchlorate ion is occupied

Table 3. Selected Bond Lengths and Angles for $[Cu_2L^{2c}](ClO_4)_2^a$

Bond Lengths (Å)			
Cu(1)−O(1)	1.940(7)	Cu(2)−O(2)	1.945(7)
Cu(1)−O(2)	2.006(7)	Cu(2)−N(4)	1.946(9)
Cu(1)−N(2)	2.013(8)	Cu(2)−O(1)	1.947(7)
Cu(1)−N(1)	2.052(8)	Cu(2)−N(3)	1.955(9)
Cu(1)−O(9)	2.427(10)		
Bond Angles (deg)			
O(1)−Cu(1)−O(2)	76.2(3)	N(1)−Cu(1)−O(9)	95.3(4)
O(1)−Cu(1)−N(2)	159.6(3)	Cu(1)−O(1)−Cu(2)	104.1(4)
O(2)−Cu(1)−N(2)	91.6(3)	O(2)−Cu(2)−N(4)	93.3(4)
O(1)−Cu(1)−N(1)	90.0(3)	O(2)−Cu(2)−O(1)	77.5(3)
O(2)−Cu(1)−N(1)	165.4(3)	N(4)−Cu(2)−O(1)	167.4(4)
N(2)−Cu(1)−N(1)	100.2(3)	O(2)−Cu(2)−N(3)	165.7(3)
O(1)−Cu(1)−O(9)	104.3(3)	N(4)−Cu(2)−N(3)	97.3(4)
O(2)−Cu(1)−O(9)	92.9(3)	O(1)−Cu(2)−N(3)	93.3(3
N(2)−Cu(1)−O(9)	92.4(3)	Cu(1)−O(2)−Cu(2)	101.7(3)

[a] Numbers in parentheses are estimated standard deviations in the least significant digits.

by O9 at an axial position, at 2.427(11) Å. The Cu1 atom deviates from the basal plane by 0.207(1) Å. The Cu2 atom has a four-coordination distorted square planar arrangement with O1, O2, N3, and N4. The Cu−N distances are 1.946(9) and 1.955(10) Å. The bond angles for N3−Cu2−O2 and N4−Cu2−O1 are 165.7(4)° and 167.4(4)° respectively. The interesting feature observed here is the presence of one perchlorate and one solvent molecule at a larger distance from the Cu2 atom. The fifth and sixth coordination positions of the Cu2 atom have one acetonitrile molecule and one perchlorate ion at a larger distance from the Cu2 atom (Cu2−N5 and Cu2−O7 = 2.571(11) and 2.728(13) Å, respectively), with an N5−Cu2−O7 angle of 177.5(4)°. The structural analysis indicates that the two metal ions in the binuclear complexes are present in the same macrocycle, because the second metal also prefers to be encapsulated in the phenolic oxygen compartment, leaving the ether oxygen compartment free. The acetonitrile molecules found in the crystal are not coordinated to the Cu(II) ion; they occupy the crystal lattice as free molecules.

3.4. Spectral Studies. IR spectra of the complexes show a ν(C═N) peak[20] at 1620−1630 cm^{-1}. The formation of this new peak, and the disappearance of the ν(C═O) peak at 1678 cm^{-1}, in the complexes are indicative of effective Schiff's base condensation. The mononuclear complexes show peaks near 1100 and 620 cm^{-1}, which are characteristic of the uncoordinated perchlorate ion. The binuclear complexes show three peaks near 1100 cm^{-1} and one peak near 620 cm^{-1}. Among the three peaks, two peaks are due to the coordinated perchlorate ion and one peak is due to the uncoordinated perchlorate ion. The electronic spectra of the complexes were observed as three main transitions. A weak band observed in the range of 575−648 nm is due to the d−d transition of the metal ion. A moderate intensive band observed in the range of 349−375 nm is due to ligand-to-metal charge-transfer transition, and the strong band observed in the range of 268−280 nm is due to intraligand charge-transfer transition.[21] An increase in λ_{max} (red shift)[22] of the d−d transition of the Cu(II) ion in the complexes from L^{1a}

(20) Das, G.; Shukala, R.; Mandal, S.; Singh, R.; Bharadwaj, P. K.; Singh, J. V.; Whitmine, K. U. *Inorg. Chem.* **1997**, *36*, 323.

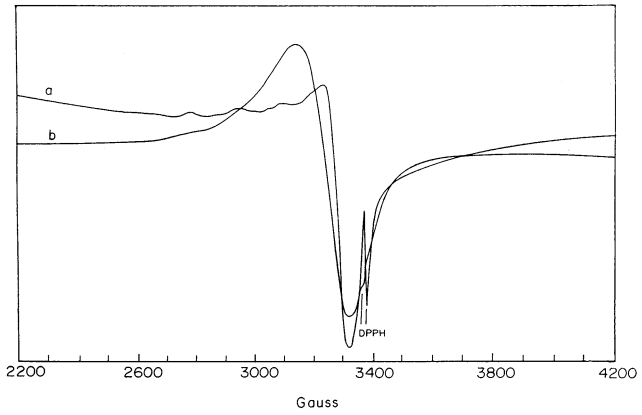

Figure 4. ESR spectra of (a) $[CuL^{1c}]ClO_4$ and (b) $[Cu_2L^{1c}](ClO_4)_2$.

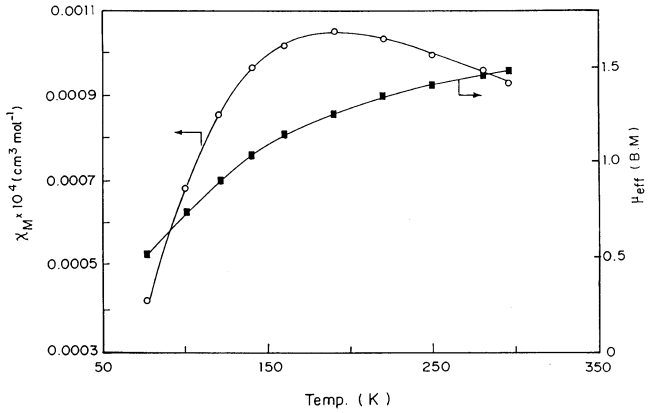

Figure 5. Temperature dependence of the magnetic properties of the complex $[Cu_2L^{1b}](ClO_4)_2$.

to L^{1c} was observed for both mono- and binuclear copper(II) complexes.

The solid-state ESR spectra of the mononuclear copper(II) complexes show four lines with a nuclear hyperfine spin of 3/2, because of hyperfine splittings. For mononuclear complexes, the observed $g_{\|}$ values fall in the range of 2.21−2.31 and $g_{\perp}$ values vary in the range of 2.03−2.09. A broad spectrum centered at $g = 2.10-2.11$ is observed for binuclear copper(II) complexes, because of the antiferromagnetic interaction between two Cu ions. Figure 4 shows the ESR spectra of the mono- and binuclear copper(II) complexes of L^{1c}.

3.5. Magnetic Studies. The probe of room-temperature magnetic studies of mononuclear copper(II) complexes resulted in magnetic-moment values (1.69−1.72 μ_B) that are very close to the spin-only value (1.73 μ_B), which is expected for complexes that have one Cu(II) ion[23] with a single unpaired electron sited in an essentially $d_{x^2-y^2}$ orbital. The observed room-temperature magnetic-moment values for binuclear copper(II) complexes are in the range of 1.45−1.55 μ_B, suggesting the presence of antiferromagnetic interaction between the two Cu(II) ions. To evaluate the singlet−triplet energy separation ($-2J$), variable-temperature magnetic study of the binuclear complexes was performed in the temperature range of 77−300 K and the experimental magnetic susceptibility values were fitted to the modified Bleany−Bowers equation[24]

$$\chi_m = \left(\frac{Ng^2\beta^2}{3kT}\right)\left[3 + \exp\left(-\frac{2J}{kT}\right)\right]^{-1}(1-P) + 0.45\left(\frac{P}{T}\right) + N_\alpha$$

in which the values of N_α and g have been fixed as 60×10^{-6} $cm^3 \cdot M^{-1}$ and 2.20, respectively. χ_m is the molar magnetic susceptibility, corrected for diamagnetism, and P is the percentage of monomeric impurities; the other symbols have their usual meaning. The $-2J$ values were evaluated by a nonlinear regression analysis in which $-2J$, P, and g are the variables. Figure 5 depicts the temperature dependence of the magnetic properties of complex $[Cu_2L^{1b}](ClO_4)_2$.

With few exceptions, magnetostructural correlations for several phenoxo-bridged[25] dicopper complexes show that the major factor that controls the exchange interactions is the Cu−O−Cu bridge angle; however, other factors,[21] such as the degree of distortion from planarity and the dihedral angle between two copper planes, also have remarkable influence on the extent of the spin−spin interaction. Generally, phenoxo-bridged coplanar dicopper complexes with $Cu-O_{ph}-Cu$ bridge angles of >99° show exchange-coupling values of >420 cm^{-1} and, for the complexes with bridge angles of <99°, the exchange interaction is less (<70 cm^{-1}).[21] Ruiz et al.[26] found that, for hydroxo- and alkoxo-bridged copper(II) complexes, the displacement (τ) O−R bond in Cu_2O_2 framework also influences the extent of exchange interaction. If there is out-of-plane displacement of R in O−R, then the antiferromagentic exchange interaction is found to be less, and for hydroxo-bridged binuclear copper(II) complexes with $\tau = 35°$, those researchers found that $-2J = 256$ cm^{-1}.[26] For the complex $[Cu_2L^{1b}](ClO_4)_2$, the $Cu-O-Cu_{(Av)}$ bridge angle is 102.9° and the observed exchange-interaction value was $-2J = 214$ cm^{-1}. The possible reason for this low value may be the deviation from coplanarity,[21] with a dihedral angle of 10.67(2)°, and the extent of out-of-plane displacement ($\tau = 39°$) of the phenyl ring from the O atom within the Cu_2O_2 framework, as Ruiz et al. already reported.[26]

3.6. Electrochemistry. Conductivity measurements[27] of mono- and binuclear copper(II) complexes in acetonitrile resulted in Λ_m values in the range of 128−160 $S \cdot cm^2 \cdot mol^{-1}$, which indicates that the complexes are of the 1:1 electrolyte type. Usually phenoxo copper complexes undergo reduction

(21) Amudha, P.; Kandaswamy, M.; Govindaswamy, L.; Velmurugan, D. *Inorg. Chem.* **1998**, *37*, 4486.
(22) Bhalla, R.; Helliwell, M.; Garner, C. D. *Inorg. Chem.* **1997**, *36*, 2944.
(23) Bottcher, A.; Elias, H.; Jager, E.; Lanffelderova, H.; Mazur, M.; Mullor, L.; Paulus, H.; Pelikan, P.; Rudolph, M.; Valko, M. *Inorg. Chem.* **1993**, *32*, 4131.
(24) Bleaney, B.; Bowers, K. D. *Proc. R. Soc. London, Ser. A* **1952**, *214*, 451.
(25) Thompson, L. K.; Mandal, S. K.; Tandon, S. S.; Bridson, J. N.; Park, M. K. *Inorg. Chem.* **1996**, *35*, 3117.
(26) (a) Ruiz, E.; Alemany, P.; Alvarez, S.; Cano, J. *J. Am. Chem. Soc.* **1997**, *119*, 1297. (b) Ruiz, E.; Alemany, P.; Alvarez, S.; Cano, J. *Inorg. Chem.* **1997**, *36*, 3683.
(27) Adam, K. R.; Anderegg, G.; Lindoy, L. F.; Lip, H. C.; McPartlin, M.; Rea, J. H.; Smith, R. J.; Tasker, P. A. *Inorg. Chem.* **1980**, *19*, 2956.

Table 4. Electrochemical Data[a] of Copper(II) Complexes in DMF Medium

complex	E^1_{pc} (V)	E^1_{pa} (V)	$E^1_{1/2}$ (V)	ΔE (mV)	E^2_{pc} (V)	E^2_{pa} (V)	$E^2_{1/2}$ (V)	ΔE (mV)	K_{con}
$[CuL^{1a}](ClO_4)$	−0.84	−0.67	−0.75	170					
$[CuL^{1b}](ClO_4)$	−0.80	−0.65	−0.72	150					
$[CuL^{1c}](ClO_4)$	−0.78	−0.63	−0.70	150					
$[CuL^{2a}](ClO_4)$	−0.87	−0.69	−0.78	180					
$[CuL^{2b}](ClO_4)$	−0.84	−0.67	−0.75	170					
$[CuL^{2c}](ClO_4)$	−0.79	−0.65	−0.72	140					
$[Cu_2L^{1a}](ClO_4)_2$	−0.90	−0.79	−0.84	110	−1.38	−1.28	−1.33	100	1.95×10^8
$[Cu_2L^{1b}](ClO_4)_2$	−0.86	−0.77	−0.81	90	−1.23	−1.15	−1.19	80	2.69×10^6
$[Cu_2L^{1c}](ClO_4)_2$	−0.83	−0.75	−0.79	80	−1.10	−1.03	−1.06	70	3.70×10^4
$[Cu_2L^{2a}](ClO_4)_2$	−0.92	−0.81	−0.86	110	−1.29	−1.19	−1.24	100	2.69×10^6
$[Cu_2L^{2b}](ClO_4)_2$	−0.85	−0.76	−0.81	90	−1.16	−1.07	−1.12	90	1.75×10^5
$[Cu_2L^{2c}](ClO_4)_2$	−0.80	−0.71	−0.76	90	−1.05	−0.97	−1.01	80	1.69×10^4

[a] Measured by cyclic voltammetry at 25 mV/s. *E* vs Ag/AgCl conditions: GC working and Ag/AgCl reference electrodes; supporting electrolyte, TBAP; concentration of complex, 1×10^{-3} M; concentration of TBAP, 1×10^{-1} M.

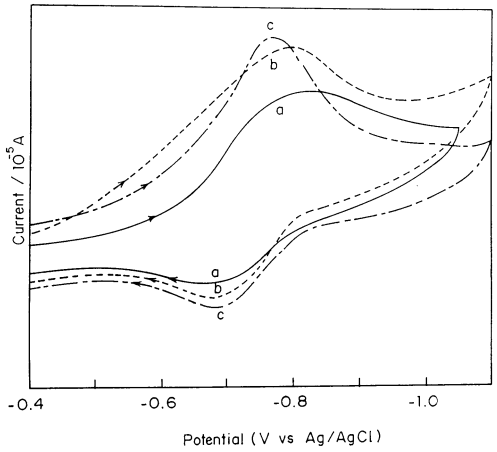

Figure 6. Cyclic voltammograms of the mononuclear copper(II) complexes (a) $[CuL^{1a}](ClO_4)$, (b) $[CuL^{1b}](ClO_4)$, and (c) $[CuL^{1c}](ClO_4)$. Concentration of each complex is 1×10^{-3} M.

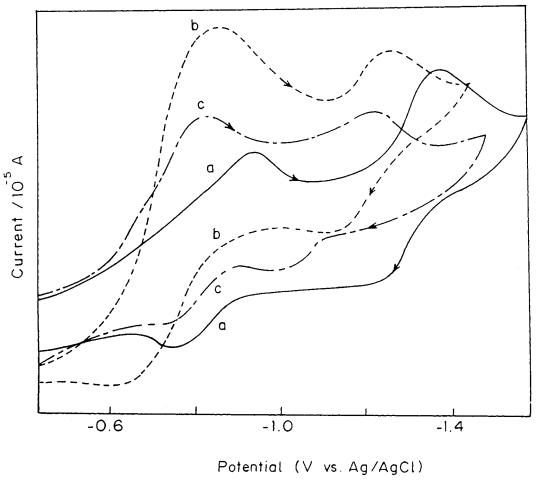

Figure 7. Cyclic voltammograms of the binuclear copper(II) complexes (a) $[Cu_2L^{1a}](ClO_4)_2$ (1×10^{-3} M), (b) $[Cu_2L^{1b}](ClO_4)_2$ (1.5×10^{-3} M), and (c) $[Cu_2L^{1c}](ClO_4)_2$ (1×10^{-3} M).

at negative potentials, because of the electronegativity and hard nature of the phenoxide atoms in the ligands.[28,29] Electrochemical properties of the complexes reported in the present work were studied by cyclic voltammetry in the potential range from 0 to −1.5 V in DMF containing 10^{-1} M TBAP, and the data are summarized in Table 4. The cyclic voltammograms for the mononuclear complexes are shown in Figure 6. Each voltammogram shows one quasi-reversible reduction wave at negative potential in the range from −0.78 to −0.87 V. Controlled potential electrolysis that is performed at potentials 100 mV more negative than the reduction wave ratifies the consumption of one electron per molecule ($n = 0.96$), and the experiment reports that the couple corresponds to one electron-transfer process. Figure 7 depicts the cyclic voltammograms for the binuclear complexes. Binuclear complexes are associated with two quasi-reversible reduction waves. The first reduction potential ranges from −0.83 to −0.92 V, and the second reduction potential lies in the range from −1.07 to −1.38 V. Controlled potential electrolysis also was performed, and the experiment reports that each couple corresponds to one electron-transfer process. So, the two redox processes are assigned as follows:

$$Cu^{II}Cu^{II} \rightleftharpoons Cu^{II}Cu^{I} \rightleftharpoons Cu^{I}Cu^{I}$$

The conproportionation constant for the equilibrium

$$Cu^{II}Cu^{II} + Cu^{I}Cu^{I} \overset{K_{con}}{\rightleftharpoons} 2Cu^{II}Cu^{I}$$

was calculated using the relationship $\log K_{con} = \Delta E/0.0591$.

It is of interest to compare the electrochemical behavior of the complexes heedfully. The reduction potential of the mononuclear copper(II) complexes of ligands L^{1a} to L^{1c} shifts toward being anodic, from −0.84 V to −0.78 V, as the number of methylene groups between imine N atoms is increased and, in turn, increases the chelate ring size. This causes more flexibility in the chelate ring[13,30−32] and tries to stabilize the copper(I) complex. The observed ΔE values for mononuclear complexes are found to be larger than the corresponding binuclear complexes, and the reason may be attributed to the occurrence of electrochemical interconversion (translocation)[11] of the reduced cation Cu(I) in mono-

(28) (a) Patterson, G. S.; Holm, R. W. *Bioinorg. Chem.* **1975**, *4*, 257. (b) Karlin, K. D.; Guitnech, Y. *Inorg. Chem.* **1987**, *35*, 219.
(29) Benzekeri, A.; Dubourdeaux, P.; Latour, J. M.; Rey, P.; Laugier, J. *J. Chem. Soc., Dalton Trans.* **1991**, 3359.
(30) Okawa, H.; Tadokora, M.; Aretake, T. Y.; Ohba, M.; Shindo, K.; Mitsumi, M.; Koikawa, M.; Tomono, M.; Fenton, D. E. *J. Chem. Soc., Dalton Trans.* **1993**, 253.
(31) Gao, E.; Bu, W.; Yang, G.; Liao, D.; Jiang, Z.; Yan, S.; Wang, G. *J. Chem. Soc., Dalton Trans.* **2000**, 1431.
(32) Connick, P. A.; Macor, K. A. *Inorg. Chem.* **1991**, *30*, 4654.

nuclear copper(II) complexes from the rigid imine nitrogen compartment (N_2O_2) to a flexible tertiary nitrogen compartment (N_2O_2), which favors the tetrahedral geometry. The larger ΔE values also indicate that the reduction process is associated with the ECE mechanism: i.e., when an input voltage is applied, the Cu(II) ion gets reduced at first to Cu(I) (electron transfer), and this reduced Cu(I) is then translocated from the rigid compartment to a flexible compartment (chemical phenomenon), which, in turn, is oxidized to Cu(II) (electron transfer) and finally reverts back to its original position (chemical phenomenon). It is also ratified that the decrease in ΔE value with the increasing chain length between two imine N atoms eases the translocation process and favors the tetrahedral geometry,[33] moving from the complexes of ligands L^{1a} to L^{1c}. In both mono- and binuclear copper(II) complexes, at low scan rates, the peaks appear to be somewhat broad. This may be due to the equilibrium binding of solvent to the Cu(II) center. The peak broadening diminishes as the scan rate increases. The interesting feature connoted for the binuclear complexes is the shifting of both first and second reduction potentials toward being anodic, from -0.90 to -0.83 V and from -1.38 to -1.21 V, respectively, as the number of methylene groups is increased. For example, the complex $[Cu_2L^{1a}](ClO_4)_2$ has $E^1_{pc} = -0.90$ V and $E^2_{pc} = -1.38$ V, the values of which are more negative in comparison to those of the complex $[Cu_2L^{1b}](ClO_4)_2$ ($E^1_{pc} = -0.86$ V, $E^2_{pc} = -1.23$ V), which, in turn, are more negative in comparison to those of the complex $[Cu_2L^{1c}](ClO_4)_2$ ($E^1_{pc} = -0.83$ V, $E^2_{pc} = -1.07$ V). Thus, as the chain length of the imine compartment increases, the entire macrocyclic ring becomes more flexible, which causes easy reduction. Thus, the large size of the cavity easily holds the reduced cation and stabilizes the formation of Cu(I) in both compartments. Another interesting feature was inferred for the binuclear copper(II) complexes from the calculation of the K_{con} values. The decrease in the value of K_{con} for the complexes of ligands L^{1a}, L^{1b}, and L^{1c} (1.95×10^7, 2.69×10^6, 1.69×10^4, respectively) and of ligands L^{2a}, L^{2b}, and L^{2c} (2.69×10^6, 1.75×10^5, 3.70×10^4, respectively) explains the phenomenon that, as the ring size increases, the stability of the mixed-valent species formed as a result of the one-electron reduction of complexes decreases. This is because the increase in ring size produces more distortion of the geometry around the metal center, and the added electron is localized in the first metal ion itself, so its impact on the other metal ion is negligible. Thus, the interaction between the two metal ions present in the distorted geometry is minimized and, hence, reduction of the second metal ion becomes easy.

An intensive speculation can be made concerning the comparison of reduction potentials of the binuclear complexes of ligands L^1 and L^2. In the case of binuclear complexes, the second reduction potential decreases uniquely as we move from the L^1 ligands that contain ethylene linkage in the tertiary nitrogen compartment to the L^2 ligands that contain propylene linkage, which is again due to an increase in flexibility, arising from a larger ring size. For example, the second reduction potentials of the binuclear complexes $[Cu_2L^{1a}](ClO_4)_2$, $[Cu_2L^{1b}](ClO_4)_2$, and $[Cu_2L^{1c}](ClO_4)_2$ are -1.38, -1.23, and -1.10 V, respectively, and they are found to be larger than the second reduction potentials of the binuclear complexes $[Cu_2L^{2a}](ClO_4)_2$, $[Cu_2L^{2b}](ClO_4)_2$, and $[Cu_2L^{2c}](ClO_4)_2$, which have potentials of -1.29, -1.16, and -1.05 V, respectively.

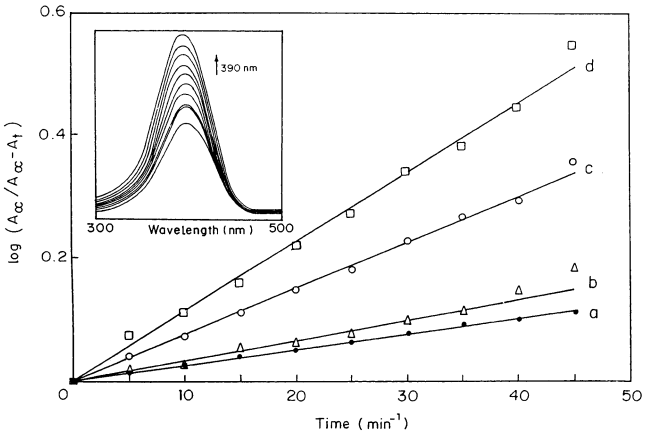

Figure 8. Catecholase activity of copper(II) complexes (a) $[CuL^{1a}]ClO_4$, (b) $[CuL^{1b}]ClO_4$, (c) $[Cu_2L^{1a}](ClO_4)_2$, and (d) $[Cu_2L^{1b}](ClO_4)_2$.

Table 5. Catecholase Activity[a] of Copper(II) Complexes

complex	rate constant, min^{-1}
$[CuL^{1a}](ClO_4)$	4.89×10^{-3}
$[CuL^{1b}](ClO_4)$	4.96×10^{-3}
$[CuL^{1c}](ClO_4)$	5.41×10^{-3}
$[CuL^{2a}](ClO_4)$	9.21×10^{-3}
$[CuL^{2b}](ClO_4)$	9.54×10^{-3}
$[Cu_2L^{1a}](ClO_4)_2$	1.27×10^{-2}
$[Cu_2L^{1b}](ClO_4)_2$	2.65×10^{-2}
$[Cu_2L^{1c}](ClO_4)_2$	4.23×10^{-2}
$[Cu_2L^{2a}](ClO_4)_2$	4.66×10^{-2}
$[Cu_2L^{2b}](ClO_4)_2$	5.32×10^{-2}

[a] Measured spectrophotometrically in a CH_3CN medium. Concentration of the complex is 1×10^{-3} M; concentration of pyrocatechol is 1×10^{-1} M.

3.7. Kinetic Studies of Oxidation of Catechol (Catecholase Activity). All the complexes synthesized so far were subjected for catecholase activity. The product *o*-quinone is considerably stable and has a strong absorbance at 390 nm. For this purpose, 10^{-3} mol·dm^{-3} solutions of complexes in acetonitrile were treated with 50 equiv of pyrocatechol in the presence of air.

The course of the reaction was followed at 390 nm for almost 45 min at regular time intervals. The slope was determined by the method of initial rates by monitoring the growth of the 390 nm band of the product *o*-quinone. A linear relationship for the initial rate and the complex concentration obtained for all the complexes shows a first-order dependence on the complex concentration for the systems.

A plot of $\log[A_\infty/(A_\infty - A_t)]$ versus time for the catecholase activity of the complexes is obtained and shown in Figure 8. The rate-constant values are also reported in Table 5. The first apparent result was that the reactivities of the complexes differ significantly. The binuclear complexes have higher

(33) Thirumavalavan, M.; Akilan, P.; Kandaswamy, M. *Inorg. Chem. Commun.* **2002**, *5*, 422.

activities than the mononuclear complexes.[34−38] For example, the binuclear complexes $[Cu_2L^{1a}](ClO_4)_2$, $[Cu_2L^{1b}](ClO_4)_2$, and $[Cu_2L^{1c}](ClO_4)_2$ have rate-constant values of 1.27×10^{-2}, 2.65×10^{-2}, and 4.23×10^{-2} min^{-1}, respectively, whereas the mononuclear complexes $[CuL^{1a}](ClO_4)$, $[CuL^{1b}](ClO_4)$, and $[CuL^{1c}](ClO_4)$ have rate-constant values of 4.89×10^{-3}, 4.96×10^{-3}, and 5.41×10^{-3} min^{-1}, respectively. The oxidation of catechol to *o*-quinone requires the presence of two metal ions in close proximity; hence, the rate-constant values of binuclear complexes are comparatively high. The catalytic activity of the complexes are found to increase as the macrocyclic ring size increases, because of the intrinsic flexibility because of which the metal ion easily gets reduced and binds with the substrate and the same was supported by both spectral and electrochemical studies. For mononuclear complexes, the observed variation in the rate-constant values is very small when compared to the binuclear complexes. The rate-constant value increases from 4.89×10^{-3} min^{-1} to 4.96×10^{-3} min^{-1} for mononuclear copper(II) complexes; for binuclear complexes, an increase from 1.27×10^{-2} min^{-1} to 2.65×10^{-2} min^{-1} is observed as we move from L^{1a} to L^{1b}.

Kinetic studies also indicate that the binuclear complexes of ligand L^2 have enhanced catalytic activities, in comparison to the activities of the complexes of ligand L^1. This can be discussed on the basis of ring size. The increase in ring size makes the system more flexible, as we have observed from electrochemical studies, and favors the catalysis phenomenon. Hence, the rate-constant values of the complexes of ligand L^2 are found to be larger than those of the complexes of ligand L^1. From Table 5, it is seen that the rate-constant value of the complex $[Cu_2L^{1a}](ClO_4)_2$ (1.27×10^{-2} min^{-1}) is less than that of the complex $[Cu_2L^{2a}](ClO_4)_2$ (4.66×10^{-2} min^{-1}).

4. Conclusion

New lateral macrobicyclic compartmental binucleating ligands, and their mono- and binuclear copper(II) complexes, have been synthesized. The complexes were subjected to spectral, electrochemical, magnetic, and catalytic studies. From these studies, it is well understood that a small variation in the ligand, in regard to factors such as chelate size and macrocyclic ring size, imposes a greater influence on electrochemical and catalytic properties of the complexes.

Acknowledgment. Financial support received by authors M.T. and P.A. from CSIR and UGC major project, sanctioned to M.K. (New Delhi), is gratefully acknowledged.

Supporting Information Available: Full crystal data and structure refinement details, atomic coordinates, equivalent isotropic displacement parameters, full interatomic distances and angles, anisotropic displacement parameters, hydrogen coordinates, and isotropic displacement parameters for the mononuclear complex $[CuL^{1a}](ClO_4)$ (CCDC No. 194128), the binuclear complex $[Cu_2L^{2c}](ClO_4)_2 \cdot 2CH_3CN$ (CCDC No. 181354), and PC-1 (CCDC No. 160252) are available from the Cambridge Crystallographic Data Centre (CCDC). Copies of this information may be obtained free of charge from The Director, CCDC, 12 Union Road, Cambridge, CB2 1EZ, U.K. (Fax: +44-1223-336033; E-mail: deposit@ccdc.cam.ac.uk; website: www.http//www.ccdc.cam.ac.uk.)

IC020633+

(34) Parimala, S.; Gita, S. N.; Kandaswamy, M. *Polyhedron* **1998**, *17*, 3445.
(35) Moore, K.; Vigee, G. S. *Inorg. Chim. Acta* **1982**, *66*, 125.
(36) Vigee, G. S.; Eduok, E. E. *J. Inorg. Nucl. Chem.* **1981**, *43*, 2171.
(37) Oishi, N.; Nishida, Y.; Ida, K. *Bull. Chem. Soc. Jpn.* **1980**, *53*, 2847.
(38) Reim, J.; Krebs, B. *J. Chem. Soc., Dalton Trans.* **1997**, 3793.